Kinetics, mechanism and thermochemistry of the gas phase reactions of CF3CH2OCH2CF3 with OH radicals: A theoretical study

ARTICLE *in* JOURNAL OF FLUORINE CHEMISTRY · MARCH 2014

Impact Factor: 1.95 · DOI: 10.1016/j.jfluchem.2014.02.009

3 AUTHORS:

Makroni Lily
North Eastern Hill University
9 PUBLICATIONS **68** CITATIONS
SEE PROFILE

Bhupesh Kumar Mishra
D. N. Government College, Itanagar, Arunac…
45 PUBLICATIONS **279** CITATIONS
SEE PROFILE

Asit K. Chandra
North Eastern Hill University
134 PUBLICATIONS **2,482** CITATIONS
SEE PROFILE

Journal of Fluorine Chemistry 161 (2014) 51–59

Contents lists available at ScienceDirect

Journal of Fluorine Chemistry

journal homepage: www.elsevier.com/locate/fluor

Kinetics, mechanism and thermochemistry of the gas phase reactions of $CF_3CH_2OCH_2CF_3$ with OH radicals: A theoretical study

Makroni Lily [a], Bhupesh Kumar Mishra [b], Asit K. Chandra [a,*]

[a] Department of Chemistry, North-Eastern Hill University, Shillong 793 022, India
[b] Department of Chemical Sciences, Tezpur University, Tezpur, Assam 784 028, India

ARTICLE INFO

Article history:
Received 25 November 2013
Received in revised form 19 February 2014
Accepted 24 February 2014
Available online 3 March 2014

Keywords:
Hydrofluoroether
M06-2X
Potential energy surface
Canonical transition state theory
Atmospheric lifetime
Global warming potentials

ABSTRACT

Theoretical investigations have been carried out on the mechanism, kinetics and thermochemistry of the gas-phase reactions between $CF_3CH_2OCH_2CF_3$ and OH radical using a newly developed DFT based M06-2X functional method. Two important H abstraction channels have been identified according to different orientations of the two H atoms bonded to same carbon atom in $-CH_2$ group, and one transition state has been located for each reaction channel. At the entry of each reaction channel, formation of pre-reactive complex indicates an indirect hydrogen-abstraction reaction. The rate coefficients were calculated for the first time over a wide range of temperature (250–1000 K) and can be expressed as a model equation: $k_{OH} = 2.55 \times 10^{-11}\exp(-(2883.7 - 387626/T)/T)\ cm^3\ molecule^{-1}\ s^{-1}$. At 298 K, our calculated rate coefficient for $CF_3CH_2OCH_2CF_3$ with OH radical $1.32 \times 10^{-13}\ cm^3\ molecule^{-1}\ s^{-1}$ is in very good agreement with the experimental result of $k_{OH} = 1.30 \times 10^{-13}\ cm^3\ molecule^{-1}\ s^{-1}$. Using a group-balanced isodesmic reaction, the standard heats of formation for $CF_3CH_2OCH_2CF_3$ and $CF_3CHOCH_2CF_3$ radical are estimated to be −365.64 and −316.84 kcal mol^{-1}, respectively. The calculated bond dissociation energy for the C–H bond in $CF_3CH(H)OCH_2CF_3$ is found to be 95.82 kcal mol^{-1} at 298 K. The atmospheric lifetime of $CF_3CH_2OCH_2CF_3$ was estimated to be around 0.272 years. The global warming potential and the main degradation process of alkoxy radical $CF_3CH(O^{\bullet})OCH_2CF_3$ are also discussed.

1. Introduction

Commercially produced compounds such as chlorofluorocarbons (CFCs), hydrofluorocarbons (HFCs) and hydrochlorofluorocarbons (HCFCs) are widely used as refrigerant, propellant, solvents and foam blowing agents, etc. These compounds have long tropospheric lifetimes (τ) and are responsible for ozone depletion in the stratosphere and also contribute to global warming [1–4]. The adverse impacts of these compounds on the environment has led to an international effort to substitute these compounds with alternative compounds which have short tropospheric lifetimes, low Ozone Depletion Potentials (ODPs) and low Global Warming Potentials (GWPs) [5–8]. Thus, major attention has been focused on replacing CFCs, HFCs and HCFCs with new generation alternatives as environmentally acceptable compounds such as short-lived Hydrofluoroethers (HFE) for various industrial applications [9,10]. In order to determine HFEs as suitable replacement for these compounds, it is important therefore, to understand the atmospheric oxidation mechanisms of HFEs and the impact on climate of their degradation products in the troposphere [11–14].

Here we focus our attention for studying the reaction of $CF_3CH_2OCH_2CF_3$ with OH radical by using quantum chemical method. Several experimental studies [15–20] have been carried out to study the kinetics of this reaction but to the best of our knowledge no theoretical studies on this reaction has been reported so far. The information obtained from experimental studies is limited primarily to overall rate coefficients and does not describe possible reaction mechanism and thermochemistry of this hydrogen to abstraction reaction. In 2007, Wilson et al. [15] determined the rate coefficients of the reaction $CF_3CH_2OCH_2CF_3$ + OH using relative rate technique and reported the Arrhenius expression: $k(T) = (3.28 \pm 0.19) \times 10^{-12}\exp[-(962 \pm 19)/T]\ cm^3\ molecule^{-1}\ s^{-1}$ with room temperature rate coefficient value of $1.30 \times 10^{-13}\ cm^3\ molecule^{-1}\ s^{-1}$. Very recently, Sengupta et al. [16] studied the same reaction using a laser photolysis-laser-induced fluorescence method over the temperature range of 298–365 K and reported the Arrhenius expression: $k(T) = (4.5 \pm 0.8) \times 10^{-12}\exp[-(1030 \pm 60)/T]\ cm^3\ molecule^{-1}\ s^{-1}$. They also reported rate coefficient at 298 K as $1.47 \times 10^{-13}\ cm^3\ molecule^{-1}\ s^{-1}$. As far as we know, the detailed reaction mechanism of the title reaction

* Corresponding author. Tel.: +91 3642722622; fax: +91 3642550486.
E-mail address: akchandra@nehu.ac.in (A.K. Chandra).

http://dx.doi.org/10.1016/j.jfluchem.2014.02.009
0022-1139/

remains is not known. Hence, in order to define the plausible mechanism and better understanding of the kinetics of the title reaction, a well-defined theoretical study is highly desirable. Therefore, as a supplement to the experiments, we here present an extensive theoretical study of the hydrogen abstraction reaction (R1) between $CF_3CH_2OCH_2CF_3$ and OH radical to understanding the title reaction more comprehensively

$$CF_3CH_2OCH_2CF_3 + OH \rightarrow CF_3CHOCH_2CF_3 + H_2O \quad (R1)$$

The DFT based M06-2X [21,22] method is utilized to investigate the mechanism and kinetics of the reaction of $CF_3CH_2OCH_2CF_3$ with OH radical over a wide temperature range of 250–1000 K. In the most stable conformer of $CF_3CH_2OCH_2CF_3$, the two hydrogen atoms in each of the two $-CH_2$ group are not equivalent and therefore two hydrogen abstraction channels are found for this reaction (discussed in detail later), namely channel 'a' and channel 'b' and both the pathways lead to the same products. The rate coefficient for each reaction channel was evaluated by using canonical transition state theory (CTST) and compared our calculated results with the available experimental values. The thermochemistry of the reaction and the heats of formation of $CF_3CH_2OCH_2CF_3$ and $CF_3CHOCH_2CF_3$ radical generated after hydrogen abstraction are also reported for the first time. We have also carried out energetic calculations of $CF_3CH_2OCH_2CF_3$ + OH reaction by using the hybrid density functional DFT at MPWB1K level [23] and make a comparative study of the MPWB1K and M06-2X results. Our calculation indicates that the M06-2X functional provide a more accurate prediction of the relative energy as compared to MPWB1K method. As a result, the M06-2X method has provided more reliable kinetic results for $CF_3CH_2OCH_2CF_3$ + OH reaction and has been primarily discussed in this manuscript. In fact, M06-2X functional is known to provide reliable kinetic and thermochemical results for atom transfer reaction [24–26].

2. Results and discussion

The lowest energy optimized structure of $CF_3CH_2OCH_2CF_3$ is shown in Fig. 1. As stated earlier, the hydrogen atoms in each of the two $-CH_2$ groups in the $CF_3CH_2OCH_2CF_3$ molecule are not equivalent due to different stereographical orientation of hydrogen atoms bonded to same carbon atom. Therefore, two TS were located for reaction (R1) for hydrogen abstraction by OH radical. The C6–H7 bond attached is shorter by almost 0.003 Å than the C1–H3 bond. The M06-2X optimized structures of reactants, two transition states and products are shown in Fig. 1 and the optimized geometrical parameters for reactants, transition states and radicals are listed in Table 1. The MPWB1K optimized structural parameters for reactants, TSs and radicals are also listed in Table 1 within parentheses. We could also locate hydrogen bonded complexes present on the reactants and products sides of the primary reaction channels (as shown in Fig. 2), indicating that the reaction between HFE and OH generally proceeds through the formation of pre- and post-reactive complexes via an indirect mechanism for each reaction channel (as shown in Fig. 3). The optimized structures of the pre-reaction (CR) and post-reaction (CP) complexes were shown in Fig. 2. Two pre-reactive complexes (CR1 and CR2) were located at the entry point of two reaction channels originated from $CF_3CH_2OCH_2CF_3$. On other hand, two CP complexes (CP1 and CP2) were found at the exit channels of the reaction. These CR complexes are formed due to weak interaction between $CF_3CH_2OCH_2CF_3$ and OH radical through C–H···O and OH···F/O hydrogen bonding, whereas the two CP complexes are

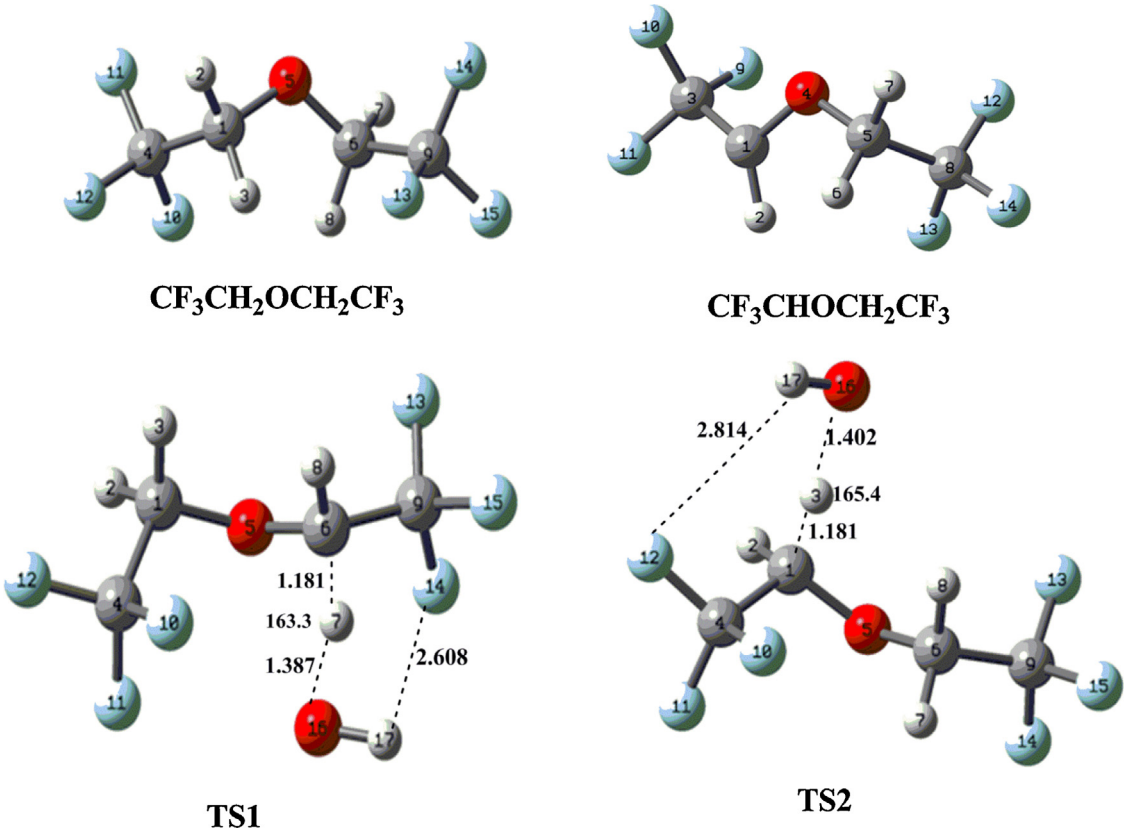

Fig. 1. Optimized structures of reactants, product and transition states at the M06-2X/6-31+G(d,p) level. Bond lengths and angles are given in Å and degrees, respectively.

Table 1
M06-2X and MPWB1K (within parentheses) optimized parameters of $CF_3CH_2OCH_2CF_3$, two transition states (TS1 and TS2) and $CF_3CH_2OCH_2CF_3$ radical. Bond lengths and angles are given in Å and degrees, respectively.

	$CF_3CH_2OCH_2CF_3$	TS1	TS2	$CF_3CHOCH_2CF_3$
C1O5/C1O4	1.4054(1.3919)	1.4033(1.3912)	1.3763(1.3639)	1.3483(1.3366)
C1C4/C1C3	1.5177 (1.5079)	1.5203(1.5109)	1.5185(1.5107)	1.4852(1.4751)
O5C6/O4C5	1.4054(1.3921)	1.3857(1.3687)	1.4159(1.4029)	1.4086(1.3957)
C6C9/C5C8	1.5177(1.5079)	1.5130(1.5034)	1.5140(1.5044)	1.5191(1.5089)
C1H2	1.0921(1.0854)	1.0909(1.0840)	1.0919(1.0845)	1.0842(1.0780)
C1H3	1.0952(1.0884)	1.0976(1.0902)	1.1806(1.2083)	
C6H7/C5H6	1.0921(1.0854)	1.1811(1.1969)	1.0942(1.0865)	1.0951(1.0880)
C6H8/C5H7	1.0952(1.0882)	1.0972(1.0896)	1.0958(1.0870)	1.0910(1.0841)
C4F10/C3F9	1.3474(1.3363)	1.3425(1.3309)	1.3452(1.3320)	1.3497(1.3392)
C4F11/C3F10	1.3366(1.3256)	1.3348(1.3235)	1.3357(1.3297)	1.3415(1.3305)
C4F12/C3F11	1.3425(1.3318)	1.3432(1.3235)	1.3444(1.3258)	1.3426(1.3318)
C9F13/C8F12	1.3474(1.3361)	1.3390(1.3293)	1.3374(1.3351)	1.3345(1.3236)
C9F14/C8F13	1.3366(1.3257)	1.3424(1.3297)	1.3388(1.3255)	1.3437(1.3326)
C9F15/C8F14	1.3425(1.3318)	1.3388(1.3275)	1.3439(1.3298)	1.3418(1.3309)
H···OH	–	1.3868(1.3305)	1.4021(1.3153)	–
C4C1O5/C3C1O4	110.24(110.67)	108.36(112.84)	114.36(114.50)	113.39(114.05)
C1O5C6/C1O4C5	110.24(116.68)	112.24(117.32)	106.67(117.86)	116.83(114.05)
O5C6C9/O4C5C8	116.48(110.58)	116.53(108.96)	117.02(107.16)	110.65(111.25)

resulted from the hydrogen bonding interaction between $CF_3CHOCH_2CF_3$ radical and H_2O molecule.

In the process of hydrogen abstraction reaction from a C–H bond, the C–H bond breaks and a new O–H bond is formed giving rise to the water molecule. As a result, the breaking C–H bond in all TS structures is found to be longer in a range of 8.4–9.1% than the observed C–H bond length in isolated $CF_3CH_2OCH_2CF_3$; whereas the forming O···H bond length is longer by 44.5–46.1% than the O–H bond length in H_2O. These structural features clearly indicate that the structure of the transition state reached early in the

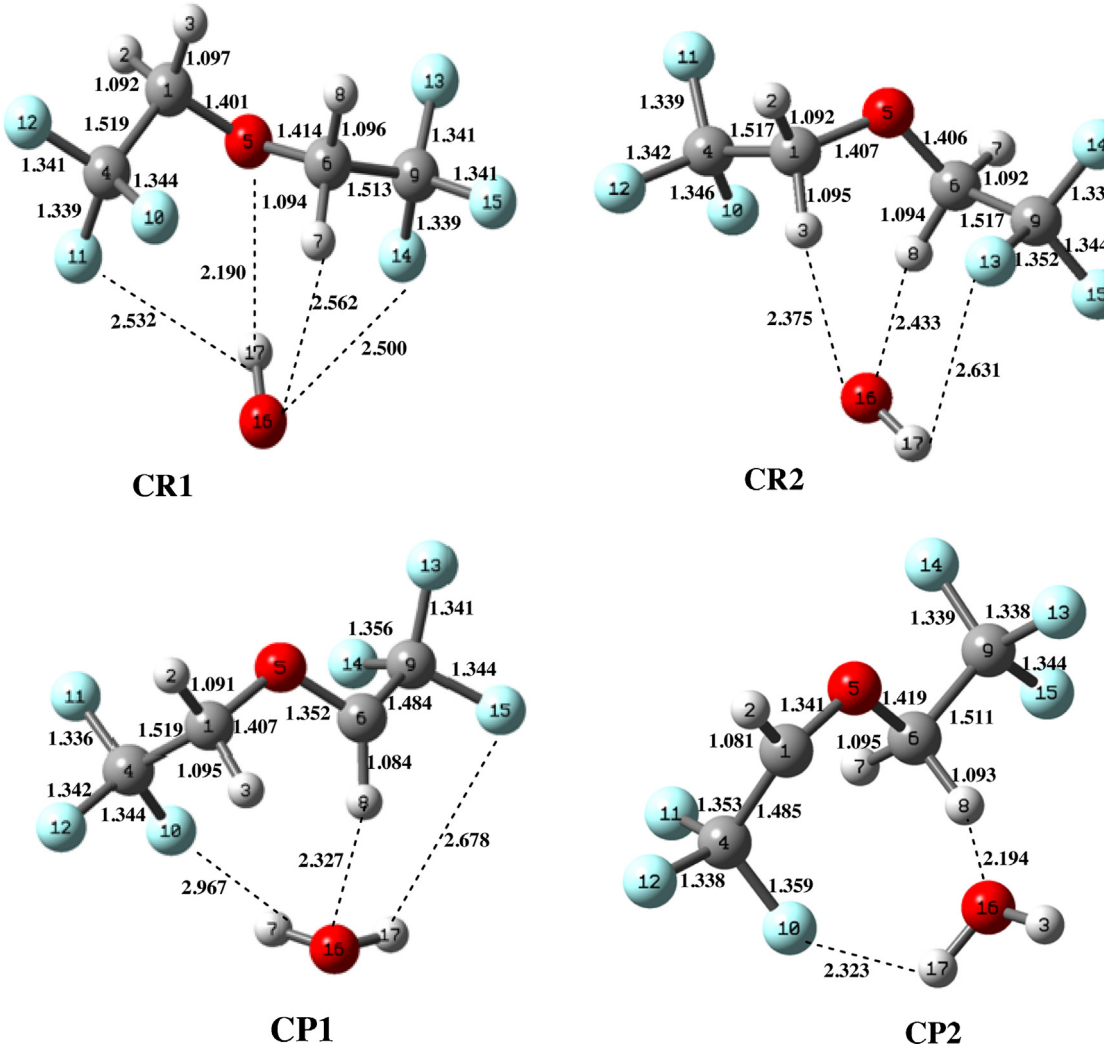

Fig. 2. Optimized structures of pre- and post-reactive complexes at the M06-2X/6-31+G(d,p) level. Bond lengths are given in Å.

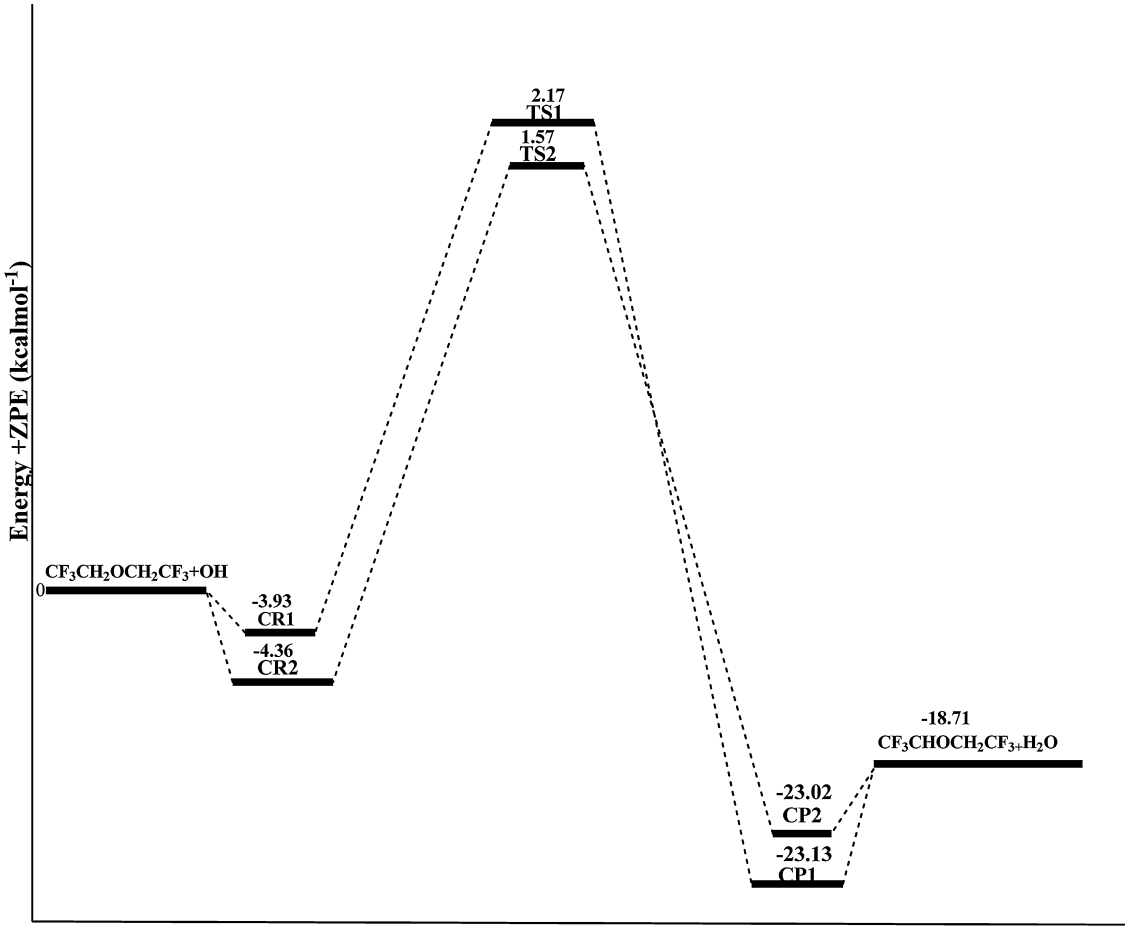

Fig. 3. Schematic potential energy profile for hydrogen abstraction reaction of $CF_3CH_2OCH_2CF_3$ + OH. Relative energies (in kcal mol^{-1}) of different species are calculated using M06-2X method.

reaction, so it resembles reactants more than products. Hence, from the thermodynamic point of view this reaction is exothermic in nature. Also, from the Hammond's postulate [27] that predicts reactant-like TS for exothermic reaction. In all the TS structures, the presence of significant hydrogen bonding interaction is found because the OH···F/O distance is seen to be significantly lower than the sum of van der Waals radii of the H and F (O) atom. The harmonic vibrational frequencies for $CF_3CH_2OCH_2CF_3$, all the transition states and product radical, pre- and post-reaction complexes are listed in Table 2. The rotational constants for all these structures are also given in Table 2. As expected, each transition state has one imaginary frequency resulting from its first order saddle point character. Applying the unrestricted spin formalism for open shell systems often has a major problem due to high spin contamination and it could lead to a significant error in barrier height estimation [28,29]. We examined the spin contamination before and after annihilation for all species involved in the title reaction. The $\langle S^2 \rangle$ values as shown in Table 2 for the doublet range from 0.7527 to 0.7589 before annihilation, whereas after annihilation, $\langle S^2 \rangle$ is 0.75 (the exact value for a pure doublet). Thus the final value of $\langle S^2 \rangle$ in our calculation shows that the wave function was not severely contaminated by states of higher multiplicity.

The relative energies (including ZPE) for all the stationary state species in reaction (R1) obtained from both the MPWB1K and M06-2X levels are given in Table 3. There are two potential hydrogen abstraction channels for the $CF_3CH_2OCH_2CF_3$ + OH reaction, whereas each channel is doubly degenerate. The M06-2X calculated barrier heights for two hydrogen abstraction channels originated from the two H-atoms of a $-CH_2$ group are 2.17 (TS1) and 1.57 kcal mol^{-1} (TS2). The same obtained from the MPWB1K calculations is almost 1 kcal mol^{-1} higher than the corresponding M06-2X results. Therefore, hydrogen abstraction from the channel $R1_b$ is kinetically more facile than channel $R1_a$. The calculated reaction enthalpies, $\Delta_r H^\circ_{298}$, of the title reactions at the MPWB1K and M06-2X levels are listed in Table 3. The reaction (R1) is exothermic in nature as expected from the character of transition states. The reaction enthalpies are −17.82 and −18.32 kcal mol^{-1}, respectively at the MPWB1K and M06-2X levels. A schematic potential energy surface of the title reactions obtained at the M06-2X level with zero-point energy (ZPE) corrections is plotted in Fig. 3. The energy of reactants is set to be zero for reference. The pre-reactive complexes (CR1 and CR2) lie below the corresponding reactants by 3.93 and 4.36 kcal mol^{-1}, whereas and post-reactive complexes (CP1 and CP2) are stabilized by 4.42 and 4.31 kcal mol^{-1} at the M06-2X level.

Our calculated BDE(C–H) are listed in Table 3. The calculated BDE(C–H) values of $CF_3CH_2OCH_2CF_3$ at M06-2X and MPWB1K methods are 95.82 and 94.52 kcal mol^{-1}, respectively. No experimental value is available for comparison, but our M06-2Xcalculated BDE value for the C–H bond is found to be in good agreement with the theoretical value of 96.39 kcal mol^{-1} by Kambanis et al. [13] and 96.87 kcal mol^{-1} by Urata et al. [30] using ANN technique.

Using a group-balanced isodesmic reactions, the heats of formation $\Delta_f H^\circ_{298}$ were calculated in which the number and types of bonds are conserved on the reactant and product sides of the reaction. It is due to the constant number of bonds of a given type, isodesmic reactions is known to predict the reaction energies quite

Table 2
Harmonic vibrational frequencies (cm^{-1}) and rotational constants (GHz, within brackets) calculated at M06-2X/6-31+G(d,p) level for different species involved in $CF_3CH_2OCH_2CF_3$ + OH reaction and pre- and post reactive complexes.

System	Frequencies (cm^{-1})	$\langle S^2\rangle$[a]
$CF_3CH_2OCH_2F_3$	38, 63, 65, 113, 155, 260, 269, 351, 363, 452, 478, 531, 532, 548, 561, 660, 683, 860, 862, 966, 994, 1043, 1179, 1235, 1238, 1253, 1263, 1331, 1336, 1357, 1359, 1448, 1462, 1482, 1504, 3103, 3110, 3176, 3178 [2.50271, 0.49077, 0.48647]	0
TS1	*1118i*, 33, 38, 54, 82, 89, 122, 161, 210, 253, 262, 317, 365, 404, 465, 533, 536, 544, 562, 656, 702, 768, 861, 893, 915, 996, 1072, 1091, 1180, 1216, 1237, 1261, 1280, 1310, 1325, 1340, 1363, 1450, 1464, 1491, 1543, 3090, 3111, 3182, 3778 [1.66103, 0.47197, 0.42854]	0.7588 (0.7596)
TS2	*966i*, 34, 37, 61, 78, 90, 122, 158, 243, 253, 271, 333, 368, 408, 470, 530, 539, 548, 563, 655, 706, 735, 858, 881, 935, 1003, 1039, 1069, 1214, 1233, 1241, 1258, 1281, 1331, 1340, 1353, 1364, 1412, 1479, 1487, 1506, 3097, 3164, 3759 [1.52977, 0.45840, 0.41321]	0.7589 (0.7601)
CR1	26, 50, 56, 71, 83, 135, 149, 163, 248, 277, 302, 359, 365, 412, 420, 465, 532, 534, 546, 563, 658, 703, 860, 881, 983, 995, 1056, 1194, 1229, 1244, 1251, 1255, 1321, 1331, 1345, 1357, 1453, 1476, 1489, 1502, 3080, 3081, 3153, 3170, 3738 [1, 65637, 0.46855, 0.42929]	0.7527 (.7533)
CR2	28, 49, 51, 58, 98, 123, 130, 155, 209, 243, 260, 270, 356, 367, 451, 486, 528, 529, 548, 559, 656, 680, 856, 860, 969, 995, 1042, 1175, 1223, 1234, 1248, 1260, 1325, 1331, 1355, 1361, 1449, 1462, 1482, 1508, 3103, 3110, 3172, 3173, 3775 [1.55444, 0.48566, 0.43115]	0.7528 (0.7528)
CP1	25, 46, 69, 75, 112, 151, 158, 177, 228, 235, 276, 285, 361, 400, 412, 458, 523, 531, 550, 568, 653, 665, 713, 863, 905, 995, 1100, 1155, 1200, 1238, 1246, 1281, 1319, 1 338, 1366, 1449, 1488, 1522, 1619, 3101, 3183, 3255, 3870, 3987 [1.42668, 0.51778, 0.44783]	0.754 (0.7544)
CP2	28, 40, 49, 80, 92, 116, 130, 146, 167, 187, 192, 234, 271, 368, 382, 386, 465, 480, 538, 550, 570, 594, 664, 737, 867, 904, 1002, 1053, 1145, 1222, 1231, 1247, 1254, 1333, 1351, 1357, 1481, 1508, 1523, 1601, 3095, 3169, 3284, 3874, 3997 [1.38687, 0.48600, 0.42820]	0.7540 (0.7541)
OH	3757 [559.895066]	0.7528 (0.7528)
H_2O	1653, 3981, 4103 [845.28063, 424.22886, .46535]	0

[a] Values within parentheses correspond to the $\langle S^2\rangle$ values at the HF/6-311G (d,p) level.

accurately even with relatively cheap theoretical methods. Hence, this property makes isodesmic reactions a valuable tool for the prediction of the heat of formation of unknown organic compounds. The enthalpies of formation ($\Delta_f H^\circ_{298}$) for species involved in a chemical reaction is required to understand the thermochemistry of that reaction and also for accurate modeling of other chemical reactions involving the same species. The $\Delta_f H^\circ_{298}$ value of $CF_3CH_2OCH_2CF_3$ was determined by using the following two isodesmic reactions at M06-2X levels:

$$CF_3CH_2OCH_2CF_3 + 2CH_4 \rightarrow CH_3OCH_3 + 2CH_3CF_3 \quad (R2)$$

$$CF_3CH_2OCH_2CF_3 + 2CH_4 + H_2O \rightarrow 2CH_3OH + 2CH_3CF_3 \quad (R3)$$

The standard gas-phase enthalpies of formation for $CF_3CH_2OCH_2CF_3$ molecule was estimated from the calculated heats of reactions and the known experimental standard heats of formation for the other species involved in two isodesmic reactions (R2) and (R3) using M06-2X method. The experimental $\Delta_f H^\circ_{298}$ values for CH_4: −17.83 kcal mol^{-1}; CH_3OCH_3: −44.0 kcal mol^{-1}; CH_3CF_3: −179.1 kcal mol^{-1}; CH_3OH: −48.04 kcal mol^{-1}; H_2O: −57.80 kcal mol^{-1} and OH: 9.32 kcal mol^{-1} were taken from Ref. [31] to evaluate the required enthalpies of formation. Our calculated $\Delta_f H^\circ_{298}$ values are reported in Table 4. The average $\Delta_f H^\circ_{298}$ value of $CF_3CH_2OCH_2CF_3$ obtained from the two isodesmic reactions (R2) and (R3) amount to −365.64 kcal mol^{-1} at the M06-2X level. Once the $\Delta_f H^\circ_{298}$ value for $CF_3CH_2OCH_2CF_3$ is known, the $\Delta_f H^\circ_{298}$ values for the radical $CF_3CHOCH_2CF_3$ generated from hydrogen abstraction reaction can easily be calculated from our calculated heats of reaction values from (R1) and the known experimental heats of formation values for OH radical and H_2O. The calculated $\Delta_f H^\circ_{298}$ value for $CF_3CHOCH_2CF_3$ radical is −316.84 kcal mol^{-1} at the M06-2X level. These data are not available in the literature and can therefore be useful for further thermochemical and kinetic modeling of reaction involving these species.

Table 3
Relative energies (ΔE_{rel} in kcal mol^{-1} including ZPE) for all species involved in $CF_3CH_2OCH_2CF_3$ + OH reaction. Reaction enthalpy ($\Delta_r H^\circ_{298}$ in kcal mol^{-1}), and C–H bond dissociation enthalpy D°_{298} (for $CF_3CH_2OCH_2CF_3$ at 298 K) at the MPWB1K and M06-2X levels of theory.

	MPWB1K	M06-2X
ΔE_{rel}		
$CF_3CH_2OCH_2CF_3$ + OH	0	0
CR1	−1.51	−3.93
CR2	−2.40	−4.36
TS1	3.29	2.17
TS2	2.57	1.57
CP1	−23.07	−23.13
CP2	−20.34	−23.02
$\Delta_r H^\circ_{298}$		
R1	−17.82	−18.32
D°_{298}		
$CF_3C(-H)HOCH_2CF_3$	94.52	95.82

2.1. Rate coefficient calculation

The rate coefficients for hydrogen abstraction reaction were calculated using the canonical transition state theory (CTST) [32]

$$k(T) = \sigma_r \Gamma(T) \frac{k_B T}{h} \frac{q_{TS}(T)}{q_{HFE}(T) q_{OH}(T)} e^{-\Delta E_0/RT} \quad (1)$$

where $q_x(T)$ represents the partition function for the species x (TS, HFE, OH) at temperature T, k_B is the Boltzmann constant, ΔE_0 is the barrier height including ZPE and σ_r is the degeneracy of each

Table 4
Heats of formation ($\Delta_r H^\circ_{298}$ in kcal mol^{-1}) values of $CF_3CH_2OCH_2CF_3$ molecule and $CF_3CH_2OCH_2CF_3$ radical calculated from isodesmic reactions (R2) and (R3) at 298 K.

Species	Reaction	$\Delta_r H^\circ_{298}$
$CF_3CH_2OCH_2CF_3$	(R2)	−365.95
$CF_3CH_2OCH_2CF_3$	(R3)	−365.32
	Average	−365.64
$CF_3CHOCH_2CF_3$	(R2)	−317.15
$CF_3CHOCH_2CF_3$	(R3)	−316.52
	Average	−316.84

reaction channel. $\Gamma(T)$ is the tunneling correction factor for taking care of tunneling contribution in H-abstraction reaction and it is simply interpreted as the ratio of quantum mechanical rate over classical mechanical rate [33]. The tunneling correction $\Gamma(T)$ was estimated by using the Eckart's unsymmetrical barrier method [33,34]. All vibrational modes, except for the lowest vibrational mode, were treated quantum mechanically as separable harmonic oscillators, whereas for the lowest-frequency mode, the partition function was evaluated by the hindered-rotor approximation proposed by Truhlar's group [35,36]. Using Truhlar's procedure [36] the q^{HIN}/q^{HO} ratio was found to be close to unity. Furthermore, the rotation of OH in TS is suppressed due to hydrogen bonding. In the calculation of the electronic partition functions, the two electronic states of the OH radicals were included, with a 139.7 cm^{-1}splitting in the $^2\Pi$ ground state [37].

The IRC calculation predicts the existence of complexes at the entrance and exit channels of the reaction ($R1_a$ and $R1_b$) and therefore the reaction $CF_3CH_2OCH_2CF_3 + OH$ proceeds via an indirect mechanism. The existence of these intermediates at the entry and exit channels of the reactions can have significant influence on the reaction rate. We have followed the procedure proposed by Singleton and Cvetonovoic [38] for taking into consideration the effect of pre- and post-reactive complex on reaction kinetics. The reaction followed a path where two reactants (HFE and OH) first form a weak complex (HFE···OH):

$$HFE + OH \leftrightarrow HFE\cdots OH \rightarrow \text{products} \quad (2)$$

If k_f and k_r are the rate coefficients for the forward and reverse reactions of the first step (complex formation), respectively and k_1 the rate coefficient for the second step, then a steady state analysis and using the argument of Singleton and Cvetonovoic [38] and others [34,39], one can express the rate coefficient k as

$$k = \frac{k_f k_1}{k_r} = \left(\frac{A_f A_1}{A_r}\right) e^{-(E_f + E_1 - E_r)/RT} = \Gamma(T)\frac{k_B T}{h}\frac{Q_{TS}}{Q_R} e^{-(E_{TS} - E_R)/RT} \quad (3)$$

where *A*s are the pre-exponential factors and *E*s are the respective barrier heights. Although the final TST expression appears to be similar as Eq. (1) irrespective of the formation of pre-reactive complex, but the formation of pre- and post-reaction complex modifies the shape of potential energy surface for the reaction and hence affects the tunneling factor $\Gamma(T)$ As a result, the rate coefficient is seen to increase at lower temperature as compared to the rate coefficient value for direct reaction from reactants to products due to greater tunneling factor. Hence, tunneling significantly lowers the effective activation energies, especially at low temperatures [40].

The rate coefficients for reaction (R1) is calculated by using the canonical transition state theory (TST) expression (Eq. (1)) and Eckart's unsymmetrical barrier method for tunneling correction in a wide range of temperature 250–1000 K. As shown in Fig. 3, $CF_3CH_2OCH_2CF_3 + OH$ reactions pass through two different channels $R1_a$ and $R1_b$ and goes through TS1 and TS2, respectively. The contribution from each of these two channels needs to be taken into account while calculating the total rate coefficient (k_{OH}) for the $CF_3CH_2OCH_2CF_3 + OH$ reaction. The total rate coefficient (k_{OH}) is therefore obtained from the addition of rate coefficients for the two channels: $k_{OH} = k1_a + k1_b$. At 298 K, our calculated k_{OH} value using M06-2X barrier heights is 1.32×10^{-13} cm^3 $molecule^{-1}$ s^{-1} which is in very good agreement with the experimental value of 1.30×10^{-13} and 1.47×10^{-13} cm^3 $molecule^{-1}$ s^{-1} reported by Wilson et al. [15] and Sengupta et al. [16], respectively. The rate coefficient obtained from the MPWB1K results is significantly lower than the M06-2X and experimental value owing to greater barrier height for hydrogen abstraction. The rate coefficients $k1_a$ and $k1_b$ and total rate coefficients (k_{OH}) values calculated at M06-2X level within a range of temperature are given in Table 5. Temperature variations of k_{OH} results obtained at M06-2X level along with the experimental results are shown in Fig. 4.

Table 5
Rate coefficients values (in cm^3 $molecule^{-1}$ s^{-1}) for hydrogen abstraction reactions of $CF_3CH_2OCH_2CF_3$ with OH radical and total rate coefficients (k_{OH}) values as calculated using M06-2X level.

Temperature (K)	M06-2X		
	$k1_a \times 10^{13}$	$k1_b \times 10^{13}$	$k_{OH} \times 10^{13}$
250	0.40	0.73	1.13
300	0.48	0.85	1.33
400	0.86	1.36	2.22
500	1.51	2.16	3.67
600	2.48	3.29	5.77
700	3.85	4.80	8.65
800	5.67	6.75	12.42
900	8.02	9.20	17.22
1000	10.98	12.21	23.19

The Arrhenius equation obtained from the calculated k_{OH} value in the temperature range of 298–450 K: $k(T) = 1.26 \times 10^{-12}$ $\exp(-675/T)$. The Arrhenius parameters in this temperature range can be compared to that was predicted from the experimental results by Wilson et al. [15]: $k(T) = 3.28 \times 10^{-12}$ $\exp(-962/T)$. However, our calculated pre-exponential factor and E_a/R value are found to be somewhat lower than that were obtained from the experimental values. These results of our work along with the available other experimental results are listed in Table 6 for further comparison.

It should be mentioned that although rate coefficients at lower temperature range are fitted in Arrhenius equation, but significant non-Arrhenius behavior, especially at lower temperature range can be observed due to tunneling and the existence of multiple channels. Therefore, temperature-dependent rate coefficient for $CF_3CH_2OCH_2CF_3 + OH$ reaction in wide temperature range (250–1000 K) is better to be described by a three parameter model equation proposed by Zheng and Truhlar [41]

$$k = C\exp\left[-\left(D_1 - \frac{D_2}{T}\right)/RT\right] \quad (4)$$

where C, D_1 and D_2 are fitting parameters ($D_1 > 0$ and $D_2 > 0$), and R is gas constant. The units of C, D_1 and D_2 in the present case are cm^3 $molecule^{-1}$ s^{-1}, kcal mol^{-1} and K kcal mol^{-1}, respectively.

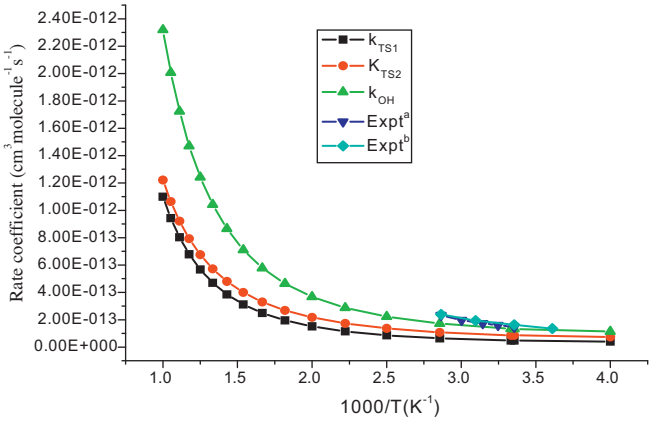

Fig. 4. Rate coefficients of hydrogen abstraction reactions from two channels (TS1 and TS2) and total rate coefficients of $CF_3CH_2OCH_2CF_3$ with OH radical at 298 K and comparison with available experimental results. [a]Ref. [16]; [b]Ref. [18].

Table 6
Comparison of experimental results with calculated results for the reaction of $CF_3CH_2OCH_2CF_3$ with OH radical at room temperature.

T (K)	A-Factor (cm^3 $molecule^{-1}$ s^{-1})	E/R (K)	$k \times 10^{13}$ (cm^3 $molecule^{-1}$ s^{-1})	Reference
298–365	$(4.5 \pm 0.8) \times 10^{-12}$	1030 ± 60	(1.47 ± 0.03)	Sengupta et al. [16]
268–409	$(3.28 \pm 0.19) \times 10^{-12}$	962 ± 19	1.31	Wilson et al. [15]
298	n/a	n/a	(1.51 ± 0.24)	Oyaro et al. [17]
277–298	$2.32^{+0.46}_{-0.41} \times 10^{-12}$	790 ± 47	$1.63 \pm 0.9)$	Orkin et al. [18]
298	n/a	n/a	0.103	Urata et al. [19]
298	n/a	n/a	1.01 ± 0.15	Sullivan et al. [20]
298	1.23×10^{-12}	678.86	1.32	This work

From above Eq. (4), the activation energy, E_a is given by:

$$E_a = \left(D_1 - \frac{2D_2}{T}\right) \quad (5)$$

The M06-2X calculated rate coefficient values for the reaction between $CF_3CH_2OCH_2CF_3$ with OH radical in the temperature range of 250–1000 K is fitted in the model Eq. (4) and found to be well described by the following equation:

$$k_{OH} = 2.55 \times 10^{-11} \exp(-(2883.7 - 387626/T)/T) \quad (6)$$

The value of activation energy, E_a for H-abstraction from $CF_3CH_2OCH_2CF_3$ by OH radical calculated from Eq. (5) is 0.56 kcal mol^{-1} at 298 K.

2.2. Atmospheric implications

2.2.1. Atmospheric lifetime

The atmospheric lifetime of $CF_3CH_2OCH_2CF_3$ (τ_{eff}) can be estimated by assuming that its removal from the atmosphere occurs primarily through the reaction with OH radicals. Then τ_{eff} can be expressed as [42]:

$$\tau_{eff} \approx \tau_{OH}$$

where $\tau_{OH} = (k_{OH} \times [OH])^{-1}$ and [OH] is the global average OH radical concentration in atmosphere. Taking the global average atmospheric OH radical concentration of 8.8×10^5 molecules/cm^3 and k_{OH} value at 298 K as 1.32×10^{-13} cm^3 $molecule^{-1}$ s^{-1}, the atmospheric lifetime of $CF_3CH_2OCH_2CF_3$ is estimated to be 0.272 year which is in very good agreement with the experimentally reported atmospheric lifetime of $CF_3CH_2OCH_2CF_3$ with respect to the reaction with OH radical, by Orkin et al. [18] (0.294 year), Kambanis et al. [13] (0.30 year) and by Sengupta et al. [16] (0.35 year).

2.2.2. Global warming potentials (GWPs)

Global warming potentials [43,44] of $CF_3CH_2OCH_2CF_3$ are predicted from density functional theory computations at the M06-2X/6-31+G(d,p) level based on the time-integrated radiative forcing from the instantaneous emission of 1 kg of a compound relative to that of 1 kg of a reference gas (CO_2) [45–47]. Then GWPs of specific species is generally estimated relative to the reference species (CO_2) information using the following equation:

$$GWP_i = \frac{a_i \int_0^{TH} e^{-t/\tau} dt}{AGWP_{CO_2}}$$

where TH is the time horizon for GWP of the species considered over, a_i is the radiative forcing due to a unit increase in atmospheric concentration of species i, and t is the time horizon over which the forcing is integrated, τ is the atmospheric lifetime of a species, AGWP is the absolute global warming potential of the reference species. Using data from M06-2X/6-31+G(d,p) level of theory and the method outlined by Pinnock et al. [48], the radiative forcing was calculated by combining the vibrational frequencies (υ_k) and intensities (A_k) of HFE molecule by the relationship

$$a_i = \sum_k A_k F(\upsilon_k)$$

where a_i is the total instantaneous infrared radiative forcing (W m^{-2} $ppbv^{-1}$), $F(\upsilon_k)$ is the binned radiative forcing function per unit cross section per wave number (W m^{-2} $(cm^{-1})^{-1}$ $(cm^2$ $molecule^{-1})^{-1}$) obtained at the band center frequency (υ_k). The GWPs computed for different time horizons and the lifetimes are tabulated in Table 7. As observed from this Table, atmospheric lifetimes and GWPs of HFE studied here are relatively smaller, when compared with those of CFCs, HFCs and HCFCs. Relative to CO_2, the GWPs of $CF_3CH_2OCH_2CF_3$ on 20-year horizon and 100-year horizon are 69.39 and 21.23, respectively while relative to CO_2, the CFC-11 on 20-year horizon and 100-year horizon are 6300 and 4600, respectively [18].

2.3. Atmospheric fate of $CF_3CH_2OCH_2CF_3$

The uptake in rainwater or cloud droplets is not an important atmospheric sink for HFEs because they have a very slow rate of dissolution in water, with their uptake coefficients ranging from 10^{-6} to 10^{-8} [49] and therefore, the major atmospheric fate of the HFEs is reaction with OH radical. The H-abstraction reaction of $CF_3CH_2OCH_2CF_3$ with OH radical gives the alkyl radical $CF_3CH(^{\bullet})OCH_2CF_3$. This alkyl radical further undergo atmospheric oxidation and formed alkoxy radical $CF_3CH(O^{\bullet})OCH_2CF_3$. The degradation of volatile organic compounds (VOCs) in the atmosphere is known to proceed mostly through alkoxy radicals, and their fate is therefore of crucial importance to the understanding of atmospheric VOCs degradation mechanisms [50]. Alkoxy radicals can react in several ways. Under atmospheric conditions, the majority of alkoxy radicals can potentially undergo reaction [51–53] with O_2 resulting in a carbonyl compound and a HO_2 radical, unimolecular decomposition via β C–C scission into an alkyl radical and a carbonyl compound and unimolecular isomerization by 1,5-H migrations forming a δ-hydroxyalkyl

Table 7
Atmospheric lifetimes of $CF_3CH_2OCH_2CF_3$ and its GWPs estimated at 298 K using the results from M06-2X/6-31+G(d,p) level.

			Global warming potentials for given time horizons					
	Atmospheric lifetime (years)		This work (years)			Reported[18] (years)		
Molecule	This work	Reported	20	100	500	20	100	500
$CF_3CH_2OCH_2CF_3$	0.272	0.294	69.39	21.23	6.63	134	39	12

radical. Wallington et al. [11] studied the atmospheric fate of $CF_3CH_2OCH_2CF_3$ and reported the formation of CF_3 radical and 2,2,2-trifluoroethyl formate (CF_3CH_2OCHO) via C–C bond scission as the major route and this was interpreted in terms of percentage yield. Here we also carried out a theoretical investigation of atmospheric degradation mechanism of $CF_3CH(O^\bullet)OCH_2CF_3$ via three possible reactions using quantum chemical methods. Geometries, frequencies and energies of the radicals and the transition states leading to their decomposition have been characterized using M06-2X level theory with 6-31+G(d,p) basis set.

The loss mechanism of $CF_3CH(O^\bullet)OCH_2CF_3$ and the formation of products are estimated by taking the following three plausible decomposition channels including oxidation with atmospheric O_2 using quantum chemical method:

$$CF_3CH(O^\bullet)OCH_2CF_3 + M \rightarrow CF_3CH_2OCHO + CF_3 + M \quad (R4)$$

$$CF_3CH(O^\bullet)OCH_2CF_3 + M \rightarrow CF_3C(O)H + CF_3CH_2O^\bullet + M \quad (R5)$$

$$CF_3CH(O^\bullet)OCH_2CF_3 + O_2 \rightarrow CF_3C(O)OCH_2CF_3 + HO_2 \quad (R6)$$

The formations of the corresponding products, CF_3 radical and CF_3CH_2OCHO in reaction (R4) undergoing unimolecular decomposition via C–C bond scission has an activation barrier of 9.60 kcal mol^{-1} and endothermic by 1.71 kcal mol^{-1}. The other decomposition pathway is via C–O bond breaking (R5) to produce $CF_3CH_2O^\bullet$ radical and $CF_3C(O)H$ (2, 2, 2-trifluoroethanal). This reaction surmounts a relatively higher energy barrier of 24.40 kcal mol^{-1} in comparison to the decomposition pathway by C–C bond scission as in reaction (R4) and endothermic by 16.72 kcal mol^{-1}. Further, reaction of $CF_3CH(O^\bullet)OCH_2CF_3$ radical with atmospheric O_2 (R6) leading to the formation of $CF_3C(O)OCH_2CF_3$ is associated with very high barrier height of 39.54 kcal mol^{-1} and is exothermic by 37.82 kcal mol^{-1}. Thus, the decomposition reaction (R4) via C–C bond scission leading to CF_3 radical and CF_3CH_2OCHO having much lower energy barrier compared to the other two processes (R5) and (R6) is kinetically the most favorable one and can occur readily in the atmosphere. Thus, our quantum chemical calculations for the possible degradation pathways of the alkoxy radical predict that reaction (R4) via C–C bond scission leading to CF_3 radical and CF_3CH_2OCHO is kinetically more favorable due to lower barrier height and CF_3CH_2OCHO to be the major product. This formate CF_3CH_2OCHO molecule can also undergo further atmospheric oxidation reactions. Out of the three prominent decomposition channels, our result reveals that C–C bond scission is the dominant path for the decomposition of $CF_3CH(O^\bullet)OCH_2CF_3$ radical in the atmosphere involving the lowest energy barrier which is in accord with recent experimental findings by Wallington et al. [11].

3. Conclusions

The H-abstraction reactions of $CF_3CH_2OCH_2CF_3$ + OH systems have been studied theoretically for the first time by using DFT based M06-2X level of theory in a wide range of temperature 250–1000 K. The most stable conformer of the $CF_3CH_2OCH_2CF_3$ molecule is used for the study. The reaction is found to follow an indirect path through the formation of pre- and post-reaction complexes. Two important reaction channels have been identified for the reaction. The calculated k_{OH}=1.32 × 10^{-13} cm^3 $molecule^{-1}$ s^{-1} is in good agreement with the reported experimental results at 298 K. A three parameter model equation has been proposed to describe the rate coefficients in a wide temperature range of 250–1000 K as k_{OH} = 2.55 × 10^{-11}exp(− (2883.7 − 387626/T)/T) cm^{-3} $molecule^{-1}$ s^{-1}. The $\Delta_f H^\circ_{298}$ values for $CF_3CH_2OCH_2CF_3$ molecule and $CF_3CHOCH_2CF_3$ radical are estimated to be −365.64 and −316.84 kcal mol^{-1}, respectively. Bond dissociation enthalpy for $CF_3CH(H)OCH_2CF_3$ is calculated as 95.82 kcal mol^{-1}. Atmospheric lifetime of $CF_3CH_2OCH_2CF_3$ is estimated to be around 0.272 year. Our results confirm that the sole atmospheric fate for decomposition of $CF_3CH(O^\bullet)OCH_2CF_3$ radical is through C–C bond scission.

4. Computational method

Gaussian 09 suites of program [54] were used to carry out all the electronic structure calculations. The geometries of all the stationary points including reactants, complexes, transition states and products were optimized using M06-2X [21,22] level of theory in conjunction with the 6-31+G(d,p) basis set. The two new hybrid meta exchange-correction functional, called M06 and M06-2X hybrid meta-GGAs, as pointed out by Zhao et al. [22] is proved to be an effective DFT method for kinetic modeling and thermochemical analysis because M06 has much better performance for energies of reaction. The M06-2X functional were used to optimize all of the stationary points on the potential energy surfaces for the reaction as well as to perform the intrinsic reaction coordinate (IRC) [55,56] calculations. Each stationary point was characterized as a minimum or a saddle point through normal-mode vibrational analysis; i.e., reactants, products and reaction complexes possess all real frequencies, whereas transition states possess one and only one imaginary frequency. The zero-point energy (ZPE) corrections are also obtained at the same level of theory. IRC calculations indicate the existence of pre- and post reaction complexes for both the reaction channels as shown in Fig. 3.

Acknowledgment

BKM is thankful to University Grants Commission, New Delhi for providing Dr. D.S. Kothari Post doctoral fellowship. AKC acknowledges CSIR, New Delhi, for financial assistance through project no. 01(2494)/11/EMR-II and the Computer Centre, NEHU for providing computational facilities.

References

[1] World Meteorological Organization (WMO), Scientific Assessment of Ozone Depletion: 2002, Global Ozone Research and Monitoring project Report No. 47, World Meteorological Organization, Geneva, Switzerland, 2003.
[2] N.L. Garland, L.J. Medhurst, H.H. Nelson, J. Geophys. Res. 98 (1993) 23107–23111.
[3] A. Sekiya, S. Misaki, Proceedings of the International Conference on Ozone Protection Technologies, Baltimore, Maryland, 1997.
[4] K.G. Kambanis, Y.G. Lazarou, P. Papagiannakopoulos, Proceedings of the IV European Symposium on Polar Stratospheric Ozone, European Commission, Schliersee, Germany, 1997.
[5] T.J. Wallington, W.F. Schneider, J. Sehested, M. Blide, J. Platz, O.J. Nielsen, L.K. Christensen, M.J. Molina, L.T. Molina, P.W. Wooddridge, J. Phys. Chem. A 101 (1997) 8264–8274.
[6] G. Marchionnia, S. Petriccia, P.A. Guardaa, G. Spataroa, G. Pezzinb, J. Fluorine Chem. 125 (2004) 1081–1086.
[7] A. Sekiya, S. Misaki, J. Fluorine Chem. 101 (2000) 215–221.
[8] R. Atkinson, J. Phys. Chem. Ref. Data Monograph 2 (1994) 1–216.
[9] A. Sekiya, S. Misaki, ChemTech 26 (1996) 44–48.
[10] W.T. Tsai, J. Hazard. Mater. 119 (2005) 69–78.
[11] T.J. Wallington, A. Guschin, T.N.N. Stein, J. Platz, J. Sehested, L.K. Christensen, O.J. Nielsen, J. Phys. Chem. A 102 (1998) 1152–1161.
[12] M.P.S. Andersen, O.J. Nielsen, B. Karpichev, T.J. Wallington, S.P. Sander, J. Phys. Chem. A 116 (2012) 5806–5820.
[13] K.G. Kambanis, Y.G. Lazarou, P. Papagiannakopoulos, J. Phys. Chem. A 102 (1998) 8620–8625.
[14] L. Chen, S. Kutsuna, K. Tokuhashi, A. Sekiya, J. Phys. Chem. A 110 (2006) 12845–12851.
[15] E.W. Wilson Jr., W.A. Hamilton, H.R. Mount, W.B. DeMore, J. Phys. Chem. A 111 (2007) 1610–1617.
[16] S. Sengupta, Y. Indulkar, A. Kumar, S. Dhanya, P.D. Naik, P.N. Bajaj, Int. J. Chem. Kinet. 42 (2010) 519–525.
[17] N. Oyaro, S.R. Sellevag, C.J. Nielsen, Environ. Sci. Technol. 38 (2004) 5567–5576.
[18] V.L. Orkin, E. Villenave, R.E. Huie, M.J. Kurylo, J. Phys. Chem. A 103 (1999) 9770–9779.
[19] S. Urata, A. Takada, T. Uchimaru, A.K. Chandra, Chem. Phys. Lett. 368 (2003) 215–223.

[20] N. O'Sullivan, J. Wenger, H. Sidebottom, in: Proceedings of the 7th European Commission Symposium on Physiochemical Behaviour of Atmospheric pollutants, Venice, Italy, October, 1996.
[21] Y. Zhao, D.G. Truhlar, Theor. Chem. Acc. 120 (2008) 215–241.
[22] Y. Zhao, D.G. Truhlar, Acc. Chem. Res. 41 (2008) 157–167.
[23] Y. Zhao, D.G. Truhlar, J. Phys. Chem. A 108 (2004) 6908–6910.
[24] G. Srinivasulu, B. Rajakumar, J. Phys. Chem. A 117 (2013) 4534–4540.
[25] Ng. Maggie, D.K.W. Mok, E.P.F. Lee, J.M. Dykle, J. Comput. Chem. 34 (2013) 545–557.
[26] T.C. Dinadayalane, G. Paytakov, J. Leszczynski, J. Mol. Model. 19 (2013) 2855–2860.
[27] G.S. Hammond, J. Am. Chem. Soc. 77 (1955) 334–338.
[28] H.B. Schlegel, C. Sosa, Chem. Phys. Lett. 145 (1988) 329–333.
[29] I.S. Ignatyev, Y. Xie, W.D. Allen, H.F. Schaefer, J. Chem. Phys. 107 (1997) 141–155.
[30] S. Urata, A. Takada, T. Uchimaru, A.K. Chandra, A. Sekiya, J. Fluorine Chem. 116 (2002) 163–171.
[31] D.R. Lide, CRC Handbook of Chemistry and Physics, 89th ed., CRC Press, NY, 2008–2009.
[32] K.J. Laidler, Chemical kinetics, 3rd ed., Pearson Education, Delhi, 2004.
[33] H.S. Johnston, J. Heicklen, J. Phys. Chem. 66 (1962) 532–533.
[34] A.K. Chandra, J. Mol. Model. 18 (2012) 4239–4240.
[35] Y.Y. Chuang, D.G. Truhlar, J. Chem. Phys. 112 (2000) 1221–1230.
[36] D.G. Truhlar, J. Comput. Chem. 12 (1991) 266–270.
[37] M.W. Chase Jr., C.A. Davies, J.R. Downey Jr., D.J. Frurip, R.A. McDonald, A.N. Syverud, J. Phys. Chem. Ref. Data 14 (Suppl. 1) (1985).
[38] D.L. Singleton, R.J. Cvetonovoic, J. Am. Chem. Soc. 98 (1976) 6812–6820.
[39] V.H. Uc, I. Garcia-Cruz, A. Hernandez-Laguna, A. Vivier-Bunge, J. Phys. Chem. A 104 (2000) 7847–7850.
[40] J. Zheng, D.G. Truhlar, J. Phys. Chem. A 113 (2009) 11919–11925.
[41] J. Zheng, D.G. Truhlar, Phys. Chem. Chem. Phys. 12 (2010) 7782–7790.
[42] M.J. Kurylo, V.L. Orkin, Chem. Rev. 103 (2003) 5049–5050.
[43] P. Blowers, D.M. Moline, K.F. Tetrault, R.R. Wheeler, S.L. Tuchawena, J. Geophys. Res. Atmos. 112 (2007) D15108.
[44] P. Blowers, D.M. Moline, K.F. Tetrault, R.R. Wheeler, S.L. Tuchawena, J. Geophys. Environ. Sci. Technol. 42 (2008) 1301–1310.
[45] J.T. Houghton, G.J. Jenkins, J.J. Ephraums (Eds.), Climate Change, The IPCC Scientific Assessment, Cambridge University Press, New York, 1990.
[46] J.T. Houghton, L.G. Meira Filho, J. Bruce, H. Lee, B.A. Callander, E. Haites, N. Harris, K. Maskell (Eds.), Climate Change 1994: Radiative Forcing of Climate Change and An Evaluation of the IPCC IS92 Emission Scenarios; Intergovernmental Panel on Climate Change, Cambridge University Press, Cambridge, UK, 1995.
[47] D.J. Wuebbles, Weighing functions for ozone depletion and greenhouse gas effects on climate, Annu. Rev. Energy Environ. 20 (1995) 45–70.
[48] S. Pinnock, M.D. Hurley, K.P. Shine, T.J. Wallington, T.J. Smyth, J. Geophys. Res. 100 (1995) 23227–23238.
[49] N. Oyaro, S.R. Sellevåg, C.J. Nielsen, J. Phys. Chem. A 109 (2005) 337–346.
[50] J. Peeters, G. Fantechi, L. Vereecken, J. Atmos. Chem. 48 (2004) 59–60.
[51] R. Atkinson, Atmos. Environ. 34 (2000) 2063–2070.
[52] E.C. Tuazon, S.M. Aschmann, R. Atkinson, W.P.L. Carter, J. Phys. Chem. A 102 (1998) 2316–2320.
[53] X.-S. Hu, J.-G. Yu, E.Y. Zeng, Int. J. Quan. Chem. 113 (2013) 1128–1130.
[54] M.J. Frisch, et al., Gaussian 09, Revision C. 01, Gaussian, Inc., Wallingford, CT, 2009.
[55] H.P. Hratchian, M.J. Frisch, H.B. Schlegel, J. Chem. Phys. 133 (2010) 224101–224108.
[56] H.P. Hratchian, M.J. Frisch, J. Chem. Phys. 134 (2011) 204103–204109.